TGF afterglows: a new radiation mechanism from thunderstorms

C. Rutjes[1], G. Diniz[2], I. S. Ferreira[2], and U. Ebert[1,3]

Casper Rutjes, casper.rutjes@cwi.nl

[1]Centrum Wiskunde & Informatica (CWI), Amsterdam, The Netherlands

[2]Instituto de Física, Universidade de Brasília, Brazil

[3]Eindhoven University of Technology, Eindhoven, The Netherlands

This article has been accepted for publication and undergone full peer review but has not been through the copyediting, typesetting, pagination and proofreading process, which may lead to differences between this version and the Version of Record. Please cite this article as doi: 10.1002/2017GL075552

Thunderstorms are known to create terrestrial gamma-ray flashes (TGFs) which are microsecond-long bursts created by runaway of thermal electrons from propagating lightning leaders, as well as gamma-ray glows that possibly are created by relativistic runaway electron avalanches (RREA) that can last for minutes or more and are sometimes terminated by a discharge. In this work we predict a new intermediate thunderstorm radiation mechanism, which we call TGF afterglow, as it is caused by the capture of photonuclear neutrons produced by a TGF. TGF afterglows are milliseconds to seconds long; this duration is caused by the thermalization time of the intermediate neutrons. TGF afterglows indicate that the primary TGF has produced photons in the energy range of 10 - 30 MeV; they are nondirectional in contrast to the primary TGF. Gurevich *et al* might have reported TGF afterglows in 2011.

Keypoints:

- TGF afterglows are predicted as a new thunderstorm radiation mechanism, next to TGFs and gamma-ray glows.
- TGF afterglows produce a relocated and prolonged detectable signal, from intermediate neutrons.
- TGF afterglows might have been observed by Gurevich *et al* in 2011.

1. Introduction

Thunderstorms emit energetic radiation of different types. Best known are Terrestrial Gamma-ray Flashes (TGFs) which are microsecond-long bursts of photons that were first observed from space [*Fishman et al.*, 1994; *Briggs et al.*, 2010]; they can be accompanied by bursts of electron positron pairs [*Dwyer et al.*, 2008b; *Briggs et al.*, 2011]. On the other hand, gamma-ray glows last much longer, for minutes or even hours; they have been observed on ground, from balloons and aircraft [*McCarthy and Parks*, 1985; *Eack et al.*, 1996; *Torii et al.*, 2002; *Tsuchiya et al.*, 2007; *Adachi et al.*, 2008; *Chilingarian et al.*, 2010, 2011]. Chilingarian *et al.* call them thunderstorm ground enhancements, which refers to the fact that the detector is located on ground.

The different properties of flashes and glows have been related to different physical mechanisms. TGFs originate from cold runaway [*Gurevich*, 1961] where thermal electrons accelerate to tens of MeV in the strong electric fields of a propagating leader discharge. TGFs appear in bursts that last for microseconds to milliseconds with a temporal distribution sketched in Fig. 1; they correlate with leader propagation. Researchers have investigated how the streamer phase [*Moss et al.*, 2006; *Li et al.*, 2009; *Chanrion and Neubert*, 2010; *Köhn et al.*, 2016] or the leader phase [*Celestin and Pasko*, 2011; *Celestin et al.*, 2012; *Chanrion et al.*, 2014; *Köhn et al.*, 2014; *Köhn and Ebert*, 2015] could accelerate electrons to energies that could explain the gamma-rays as an effect of bremsstrahlung. Experimentally cold runaway has been found in pulsed discharges [*Stankevich and Kalinin*, 1967; *Kostyrya et al.*, 2006; *Tarasenko et al.*, 2008; *Shao et al.*, 2011] and during the formation of meter long laboratory sparks [*Noggle et al.*, 1968; *Nguyen et al.*, 2008; *Dwyer et al.*,

2008a; *Rep'ev and Repin*, 2008; *Cooray et al.*, 2009; *Kochkin et al.*, 2012, 2015, 2016]. Glows on the other hand would originate from relativistic runaway electron avalanches (RREA) [*Gurevich et al.*, 1992; *Dwyer*, 2003], with feedback of photons and positrons creating new avalanches [*Babich et al.*, 2005; *Dwyer*, 2007, 2012]; they evolve on the timescale of seconds to minutes and even hours, as sketched in Fig. 1 as well. Whereas lightning leaders produce TGFs, lightning is observed to terminate gamma-ray glows [*McCarthy and Parks*, 1985; *Chilingarian et al.*, 2015; *Kelley et al.*, 2015].

Here we predict a new intermediate thunderstorm radiation mechanism, which we call TGF afterglow, that evolves on the timescale of milliseconds to seconds, as also sketched in Fig. 1. In short, when photons in the TGF are energetic enough to release neutrons from air molecules by a photonuclear reaction, the neutrons have initial energies of tens of MeV and slowly cool down through collisions with nuclei of air molecules (as neutrons have no electric charge). During thermalization they can be captured again by nuclei and sometimes with the release of a high energy photon, hence in those cases reverting the photonuclear reaction.

That thunderstorms produce neutrons is observed [*Shah et al.*, 1985; *Shyam and Kaushik*, 1999; *Bratolyubova-Tsulukidze et al.*, 2004; *Gurevich et al.*, 2012; *Chilingarian et al.*, 2012; *Starodubtsev et al.*, 2012; *Toropov et al.*, 2013; *Kozlov et al.*, 2013; *Gurevich et al.*, 2015]; and the relevant generation channels have been identified [*Fleischer et al.*, 1974; *Babich*, 2006; *Babich and Roussel-Dupré*, 2007; *Babich*, 2007; *Babich et al.*, 2014] as photonuclear reactions $\gamma + {}^{14}\mathrm{N} \rightarrow \mathrm{n} + {}^{13}\mathrm{N}$, $\gamma + {}^{16}\mathrm{O} \rightarrow \mathrm{n} + {}^{15}\mathrm{O}$ and $\gamma + {}^{40}\mathrm{Ar} \rightarrow \mathrm{n} + {}^{39}\mathrm{Ar}$, with threshold energies of $\epsilon_N = 10.55$ MeV, $\epsilon_O = 15.7$ MeV and $\epsilon_{Ar} = 9.55$ MeV, respectively

[*Dietrich and Berman*, 1988]. The photonuclear cross section is maximal for photons of roughly 23 MeV, creating neutrons of roughly 13 MeV; for a further discussion of the energy spectrum of the neutrons we refer to *Babich et al.* [2010]. Electrodisintegration reactions (where electrons react with nuclei) could contribute to neutron generation as well, but their contribution is negligible [*Babich et al.*, 2014]. The simulations by *Babich et al.* [2007, 2008]; *Carlson et al.* [2010]; *Drozdov et al.* [2013]; *Köhn and Ebert* [2015] have focussed on neutron production from TGFs, with the number of neutrons produced by a typical TGF varying from 10^{12} neutrons by *Carlson et al.* [2010] to 10^{15} neutrons by *Babich et al.* [2007, 2008]. This is mainly due to different assumptions of the total number of photons and their spectrum, or of the initial electrons that create the photons by bremsstrahlung. These studies focus on the neutron emission, and we will return to them in Sec. 2. The present study addresses for the first time the prolonged and relocated gamma-ray glow generated by the nuclear capture of the neutrons during their thermalization.

Gurevich et al. [2011] have recently observed gamma-ray emissions lasting 100 to 600 ms during lightning activity, with some inner temporal structures with durations that are too long for a TGF, which on ground maximally lasts a few hundreds of microseconds. These observations might be the first measurement of TGF afterglows. We will return to these observations in Sec. 3 to illustrate how TGF afterglows would qualitatively appear in measurements.

2. Simulations

2.1. Setup of simulations

Here we present two simulations, made with the general purpose Monte Carlo code FLUKA [www.fluka.org] [*Ferrari et al.*, 2005; *Böhlen et al.*, 2014], which performs very well in the energy regime relevant for TGFs [*Rutjes et al.*, 2016], and which has state-of-the-art neutron transport and interactions [*Böhlen et al.*, 2014]. We simulate in air (78.085% N_2, 20.95% O_2 and 0.965% Ar) with the altitude dependent density profile given by the 'US Standard Atmosphere (1976)' (by the U.S. Committee on Extension to the Standard Atmosphere).

We perform both simulations within a cylindrical section of the atmosphere extending from ground up to 18 km altitude, with a radius of 12 km. Within FLUKA, this volume is partitioned into 72 horizontal slabs of 250 m thickness in altitude. Every slab is filled with a homogenous air density determined by the air density of the 'US Standard Atmosphere (1976)' at the bottom of each slab, resulting in an exponential density profile starting from 1.225 kg m^{-3} in the lowermost slab up to 0.1216 kg m^{-3} in the uppermost slab. The temperature, however, is constant and equal to 293K everywhere. Each horizontal slab interface acts as an infinitely thin virtual detector, which detects any passing particle. The output that we record at these interfaces is: the particle type and its kinetic energy, its position in the interface plane, and the time of passing.

The output allows to calculate directly the average flux through the interfaces within a time bin. The time bins are equally spaced on logarithmic scale, with edges given by 10^p s, where p ranges from -9 to 2 in steps of 0.1. The particle density at the interfaces is approximated by dividing the flux by the velocity; more precisely, for the neutrons we add the inverse square root of the kinetic energy of all particles passing the interface within

a time bin with an appropriate factor ($\sqrt{m_n/2}$). This approximation of the density is within the accuracy level of other parameters. This time averaged density is presented in different manners in Figures 2 and 3. The top panel shows these averaged densities integrated over the horizontal interfaces as a function of the discrete altitudes of these interfaces. The middle panel shows the average density as a function of radius at a given altitude. The bottom panel shows the total particle numbers in the system. Discretization artifacts in these figures are due to the discreteness of the interface altitudes and the time bins.

After the primary electron acceleration in a discharge, electrons, photons, neutrons and other TGF products move independently through the atmosphere colliding only with neutral gas molecules, hence the further evolution is linear. We therefore always start with 10^8 particles, and we can get higher particle numbers by multiplying initial, intermediate and final states by the same number. The number 10^8 is chosen as a compromise between statistical accuracy and computational demands.

As already discussed, electrons can gain high energies near leader discharges, and these electron energies are converted into photons by bremsstrahlung. A recent study by *Mailyan et al.* [2016] of 46 TGFs constrains the average number of electrons with energies above 1 MeV to approximately 2×10^{18}, with a range from 4×10^{16} to 3×10^{19}, for source altitudes above 10 km. According to *Briggs et al.* [2010]; *Marisaldi et al.* [2014] photon energies can reach up to tens of MeV. We here concentrate on the photons with energies between 10 and 30 MeV as they can create neutrons by a photonuclear interaction. *Gjesteland et al.* [2015] analyze three TGFs and estimate that the number of photons with

energy above 1 MeM varies between 10^{17} and 10^{20} under the assumption that the TGFs have started at 8 km altitude.

2.2. TGF afterglow generated by the primary TGF

Our first simulation assumes that the TGF is at 8 km altitude and directed downward. It starts with 10^8 photons with uniformly distributed energies between 10 and 30 MeV. Using the results of *Gjesteland et al.* [2015], and assuming that 1% of the photons with energy above 1 MeV have an energy above 10 MeV, we should actually consider $10^{16\pm1}$ photons above 10 MeV rather than 10^8. But as the evolution outside the TGF source is linear, we can take this into account by multiplying the result of the evolution of 10^8 photons by a factor $10^{8\pm1}$.

Fig. 2 shows the evolution as function of the logarithm of time. Photons are included only if their energy exceeds 10 keV. The presented quantities are defined in Sec. 2.1. The top panel of Fig. 2, viewed from left to right, shows first the light cone of the developing TGF as non-filled red to yellow contours. Photons moving upward have been backscattered or they are secondary, which implies that they have lost a significant amount of energy. Therefore only the primary photons (that move downward), will be energetic enough to produce neutrons; hence the neutron cloud appears only at lower altitudes in this configuration. The mean free path of the photonuclear reaciton scales with density as $\ell = \ell_0 \frac{n_0}{n}$. For the integrated density (starting at 8 km downward), the mean free path of the photonuclear cross section equals 5 km, consistent with Fig. 2.

When the neutrons are just created, their typical energy is of the order of 13 MeV (the energy of the maximum of the photonuclear cross section minus the neutron binding energy

in nitrogen nuclei); then the neutrons diffuse isotropically and cool down (the neutron energy is given in the bottom panel of Fig. 2). While cooling down, the intermediate neutrons do create some photons by inelastic scattering, visible in the top panel at around 3 km, where the TGF envelope extends longer in time than at other altitudes, but after 10^{-4} s the secondary photons produced by inelastic scattering have energies below 10 keV and are thus not shown. The time for neutron thermalization scales as $t = t_0 \frac{n_0}{n}$. We see in the bottom panel of Fig. 2 that around 3 km altitude the intermediate neutrons take 0.5 s to thermalize. Neutrons can (at any energy) be captured again, but the cross section for neutron capture increases for decreasing energy as $\sigma_{\text{capture}} \propto 1/\sqrt{E_{\text{neutron}}} \propto 1/v_{\text{neutron}}$, according to the so-called $1/v$-law (see chapter II of [*Blatt and Weisskopf*, 1979]). Because of the $1/v$-law, the rate k_{capt} of neutron capture and hence of photon production in the TGF afterglow is constant for constant air density, as $k_{\text{capt}} = v_{\text{neutron}} \sigma_{\text{capture}} n_{\text{air}} \propto \frac{n}{n_0}$. Actually, the most significant capture pathway is not producing a high energy photon, but of radiocarbon (i.e. $n + {}^{14}\text{N} \rightarrow {}^{14}\text{C} + \text{p}$). The cross section for this reaction is $\sigma_{\text{capt}} = 1.8 \times 10^{-28}$ m^2 [*Choi et al.*, 2007] at thermal velocities (0.025 eV, 2200 m/s), yielding a neutron capture rate of 15.8 s$^{-1} \frac{n}{n_0}$. The TGF afterglow timescale is thus

$$T_{\text{afterglow}} = 1/k_{\text{capt}} \approx 0.063\,\text{s} \exp\left(\frac{h}{7\,\text{km}}\right), \tag{1}$$

if one assumes an exponential air density profile with a scale height of 7 km.

The bottom panel in Fig. 2 shows the total number of photons and neutrons. This number is the domain integrated time-averaged density, as explained in Sec. 2.1. The evolution can be explained in a simple way, with three species and four rates, where we for convenience neglect the altitude (i.e., air density) dependence of the reaction rates

(as all frequencies scale as $f = f_0 \frac{n}{n_0}$). The first reaction is the absorption of high energy photons,

$$N_\gamma(t) \approx N_\gamma(0) \exp\left[-k_{\mathrm{ph-absorp}} t\right] \tag{2}$$

with the photon absorption rate $k_{\mathrm{ph-absorb}} = \mu c \approx 2 \times 10^5$ s^{-1} at STP, (where μ is the photon attenuation coefficient, for a discussion see *Rutjes et al.* [2016]). The loss due to the production of neutrons, i.e. the photonuclear reaction $k_{\mathrm{ph-nuc}} = c\sigma_{\mathrm{ph-nuc}} n_{\mathrm{air}} \approx 8 \times 10^2$ s^{-1}, can be neglected in Eq. 2 as $k_{\mathrm{ph-absorp}} \gg k_{\mathrm{ph-nuc}}$. In Fig. 2 one sees that the photon number $N_\gamma(t)$ (displayed as diamonds) first increases, as the TGF beam creates also secondary photons, which are counted in the simulation, but Eq. 2 approximates only the number of high energy photons (with energies say $\gtrsim 1$ MeV), see further discussion by *Rutjes et al.* [2016].

The photonuclear cross section for nitrogen and for photons between 10 and 30 MeV ranges from 1 mb to a peak value of 14 mb at photon energy of 23 MeV [*Oblozinskỳ*, 2000]. For the approximation of $k_{\mathrm{ph-nuc}}$ above, we took the average photonuclear cross section of nitrogen $\sigma_{\mathrm{ph-nuc}} \approx 2$ mb. The number of neutrons per TGF photon (between 10 MeV and 30 MeV) can then be approximated as $\frac{k_{\mathrm{ph-nuc}}}{k_{\mathrm{ph-absorp}}} \approx 4 \times 10^{-3}$ (consistent with the result of 4.3×10^{-3} by *Babich et al.* [2010]). One may assume that all neutrons are generated - as this is limited by the photon absorption timescale $k^{-1}_{\mathrm{ph-absorp}} \approx 5$ μs - before they start to disappear by capture, which happens with a rate of $k_{\mathrm{capt}} \approx (80\,\mathrm{ms})^{-1}$ at 3 km altitude.

As already mentioned above k_{capt} does not depend on energy, but only on altitude. For the number of intermediate neutrons this yields

$$N_n(t) \approx N_\gamma(0) \frac{k_{\mathrm{ph-nuc}}}{k_{\mathrm{ph-absorp}}} \exp\left[-k_{\mathrm{capt}} t\right] \quad \text{for } t \gg k_{\mathrm{ph-absorp}}^{-1}. \tag{3}$$

This equation is consistent with our simulated neutron number, indicated with crosses in the bottom panel of Fig. 2. For the gamma-radiation of the TGF afterglow we need to use the number of neutrons and the reaction rate from the most significant pathway producing high energy photons, i.e. $n + {}^{14}\mathrm{N} \rightarrow {}^{15}\mathrm{N} + \gamma$, which happens with a rate of $k_{\mathrm{n-ph}} = 0.7\ \mathrm{s}^{-1}$ as the cross section equals $7.98 \times 10^{-30}\ \mathrm{m}^2$ [*Choi et al.*, 2007] at thermal velocities (0.025 eV, 2200 m/s). Together this results in

$$N_{\gamma-\mathrm{TGF\,afterglow}}(t) \approx \frac{k_{\mathrm{n-ph}}}{k_{\mathrm{ph-absorp}}} N_n(t) \approx N_\gamma(0) \frac{k_{\mathrm{ph-nuc}} k_{\mathrm{n-ph}}}{k_{\mathrm{ph-absorp}}^2} \exp\left[-k_{\mathrm{capt}} t\right] \quad \text{for } t \gg k_{\mathrm{ph-absorp}}^{-1}, \tag{4}$$

where $\frac{k_{\mathrm{ph-nuc}} k_{\mathrm{ph-nuc}}}{k_{\mathrm{ph-absorp}}^2} \approx 1.3 \times 10^{-8}$, consistent with our simulated photon numbers, indicated with diamonds in the bottom panel of Fig. 2.

2.3. TGF afterglow generated by neutrons (for better statistics)

The number of simulated photons in the TGF afterglow in Fig. 2 is limited, as we started the Monte Carlo simulation with 10^8 primary photons, and as the conversion rate from photon to neutron and consecutively from neutron back to photon is low. To achieve better statistics, our second simulation starts directly with 10^8 neutrons at an altitude of 10 km. As photons with energies between between 10 and 30 MeV are converted into neutrons with a probability of about 4×10^{-3} according to our calculations and to *Babich et al.* [2010], we have to multiply our simulation results for particle numbers now with a

factor of $4 \times 10^{5\pm1}$ to simulate a TGF with $10^{16\pm1}$ primary photons in the required energy range.

The 10^8 neutrons of our simulation initially all have the most probable energy of 13 MeV, and they are directed downwards, but they rapidly transit to isotropic diffusion. Fig. 3 presents the evolution of neutrons and photons in a similar manner as Fig. 2, but now focused on the TGF afterglow after 1 ms. Apart from the better statistics of neutron to photon conversion, there are major differences to the earlier simulation. As the air density $n_{\rm air}$ is 2.2 times lower, the neutrons cool down 2.2 times more slowly, and they spread 2.2 times more widely, hence the TGF afterglow is much more extended in space and duration. At the altitude of 10 km it lasts for more than 1 s, as the rate constant $k_{\rm capt}$ in Eq. (3) is now $k_{\rm capt} \approx 5$ s^{-1}.

The statistics of Fig. 3 are much better than those of Fig. 2, but unfortunately the simulated box (see Sec. 2.1) was too small to keep all particles. The top panel clearly indicates that many particles leave the system at its upper border at 18 km altitude. Therefore the normalization rates of Eqs. (2-4) do not apply in the same fashion, so we rescaled them to fit the data. The decay rate of particles, however, with a rate constant of 5/s at 10 km altitude represents a good fit.

2.4. The predicted detector signal

One question is whether the predicted TGF afterglow will be measurable above the cosmic background radiation. Figures 2 and 3 show that it will be hard to detect a TGF afterglow at sea level, if the neutrons are created above 3 km. We have calculated the predicted detector signal of the TGF afterglows for the simulation of Fig. 2 at 3 km

altitude, and for the simulation of Fig. 3 at 10 km altitude. The detector is the one of *Gurevich et al.* [2011] with an area of 475 cm^2, and we used a temporal bin size of 200 μs as in their published plots. We assume that it is hit by 2 $cm^{-2}s^{-1}$ or 9 $cm^{-2}s^{-1}$ cosmic background photons with energy above our threshold of 10 keV at 3 or 10 km altitude, based on *Bazilevskaya et al.* [2008]. This Poisson-distributed background is added to the signal in Fig. 4.

As discussed above, the particle numbers of our simulation are orders of magnitude lower than in a real TGF. The statistics of our simulation are corrected to 10^{16} initial photons between 10 and 30 MeV. Obviously, the TGF afterglow can clearly be detected above the cosmic background radiation. The signal would be even more conspicuous for TGFs containing 10^{17} or 10^{18} photon, above 10 MeV. It is important to remark that photons decay with a rate of $k_{\mathrm{ph-absorp}} = (5\,\mu\mathrm{s})^{-1}$ at STP, or with $(7\,\mu\mathrm{s})^{-1}$ and $(15\,\mu\mathrm{s})^{-1}$ at 3 km and 10 km, respectively. Thus the TGF signal from the simulation of Fig. 2 is only visible as a point at $t = 0$ ms in Fig. 4, and the duration of the TGF afterglow is just the life-time of the neutrons, as explained with Eq. (4).

2.5. Summary of predictions for TGF afterglows

We have predicted a new thunderstorm radiation mechanism, the TGF afterglow. It is formed by the photonuclear production of neutrons by the TGF, neutron propagation and cooling and the inverse reaction that creates gamma-rays again. TGF afterglows are thus a signature of gamma-rays above 10 to 30 MeV. A TGF afterglow can be distinguished from TGFs or gamma-ray glows by the following criteria:

1. **Duration:** A TGF lasts not longer than 200 μs, or possibly 600 μs depending on the interpretation of some observations as one or several flashes. A gamma-ray glow lasts for seconds or more, see Fig. 1. A TGF afterglow lasts for 60 to 600 ms depending on the atmospheric altitudes crossed by the intermediate neutrons acting as their source, see Eq. (1). See also Fig. 1 for illustration.

2. **Signal shape:** Neutron and photon signal appear suddenly and decay in time, compared to the photon and neutron signal in a gamma-ray glow which first swells and then decays.

3. **Correlation with fast field changes:** TGF afterglows are created by TGFs which are triggered by leader propagation and related to fast electric field changes. Gamma-ray glows are seen before a discharge and can be terminated by one.

4. **Photon isotropy:** The photons of a TGF afterglow are fairly isotropic, in contrast the beams produced either in a TGF of in a gamma-ray glow by the beamed motion of electrons and their beamed gamma-ray emission by bremsstrahlung).

5. **Energy range:** The photon energy does not exceed the photonnuclear energy of $\epsilon_N \approx 10$ MeV for nitrogen, compared to many tens of MeV in a gamma-ray glow or TGF.).

3. Possible observations and outlook

As already mentioned in the introduction, *Gurevich et al.* [2011] have reported gamma-ray emissions lasting for 0.1 to 0.6 s. Clearly, the duration is significantly longer than any TGF detected or simulated, which should disappear within a millisecond, but the signals reported by *Gurevich et al.* [2011] are many orders longer. They occurred during

the full duration of an atmospheric discharge at the Tien-Shan Cosmic Ray station at 3.3 to 3.9 km altitude, within the Tien-Shan mountains that reach up to almost 7.5 km altitude. *Gurevich et al.* [2011] found that the temporal distribution of gamma-radiation intensity in a burst is quite non-uniform, with some time structures on the scale of ms strongly correlated with an electric field change during the discharge. Based on duration only, the measurements fall in the regime of TGF afterglows, see Fig. 1 for illustration.

To illustrate how TGF afterglows would qualitatively appear in measurements, we added one event from [*Gurevich et al.*, 2011] to Fig. 4, see panel C and D. The measured gamma-ray counts in panel C appear suddenly at $t = 0$ ms, simultaneous with a fast field variation given in panel D, after which it decays in time. This measured structure in panel C, from 0 ms to 200 ms, shows similarities to our simulated TGF afterglow at 3 km. But, the observations are probably not produced by the specific TGF that we simulated (a TGF starting at 8 km and directed vertically downwards), there could be other scenarios (different altitude, orientation, opening angle and photon spectrum), in addition also the number of photons per TGF varies by an order of magnitude.

The measurements of *Gurevich et al.* [2011] show also structures that would not fit in the description of a TGF afterglow. Namely, structures that first swell and then decay, centered around one or multiple fast field variations. An example of such a structure is also seen in panel C and D, between 200 ms to 300 ms. We speculate that it fits in the description of a gamma-ray glow, but a transient one with a much shorter life-time than typically measured. It could be the result of field development by previous

partial discharges, producing a transient patch of air with an electric field above runaway breakdown, until the patch itself is discharged by a leader.

There may be more candidates of gamma-ray observations from thunderstorms which are actually TGF afterglows. We have summarized discriminators in Sec. 2.5 to search for TGF afterglows and we invite other researches to look for their signatures in their millisecond-timescale gamma-ray measurements.

Acknowledgments. C.R. acknowledges funding by FOM project Project No. 12PR3041. G.D. is supported by the Brazilian agencies CAPES and CNPq. Data (e.g. cross sections) used in this work were provided by the software package FLUKA (see Sec. 2.1) available at www.fluka.org.

References

Adachi, T., Y. Takahashi, H. Ohya, F. Tsuchiya, K. Yamashita, M. Yamamoto, and H. Hashiguchi (2008), Monitoring of lightning activity in southeast asia: Scientific objectives and strategies, *Kyoto Working Papers on Area Studies: G-COE Series*.

Babich, L. (2007), Neutron generation mechanism correlated with lightning discharges, *Geomagnetism and Aeronomy*, *47*(5), 664–670.

Babich, L., E. Donskoy, I. Kutsyk, and R. Roussel-Dupré (2005), The feedback mechanism of runaway air breakdown, *Geophysical research letters*, *32*(9).

Babich, L., A. Y. Kudryavtsev, M. Kudryavtseva, and I. Kutsyk (2008), Atmospheric gamma-ray and neutron flashes, *Journal of Experimental and Theoretical Physics*, *106*(1), 65–76.

Babich, L. P. (2006), Generation of neutrons in giant upward atmospheric discharges, *JETP letters*, *84*(6), 285–288.

Babich, L. P., and R. A. Roussel-Dupré (2007), Origin of neutron flux increases observed in correlation with lightning, *Journal of Geophysical Research: Atmospheres*, *112*(D13).

Babich, L. P., A. Y. Kudryavtsev, M. Kudryavtseva, and I. Kutsyk (2007), Terrestrial gamma-ray flashes and neutron pulses from direct simulations of gigantic upward atmospheric discharge, *JETP Letters*, *85*(10), 483–487.

Babich, L. P., E. I. Bochkov, I. M. Kutsyk, and R. A. Roussel-Dupré (2010), Localization of the source of terrestrial neutron bursts detected in thunderstorm atmosphere, *Journal of Geophysical Research: Space Physics*, *115*(A5).

Babich, L. P., E. I. Bochkov, I. M. Kutsyk, and H. K. Rassoul (2014), Analysis of fundamental interactions capable of producing neutrons in thunderstorms, *Phys. Rev. D*, *89*, 093,010, doi:10.1103/PhysRevD.89.093010.

Bazilevskaya, G. A., I. G. Usoskin, E. O. Flückiger, R. G. Harrison, L. Desorgher, R. Bütikofer, M. B. Krainev, V. S. Makhmutov, Y. I. Stozhkov, A. K. Svirzhevskaya, N. S. Svirzhevsky, and G. A. Kovaltsov (2008), Cosmic Ray Induced Ion Production in the Atmosphere, *Space Sci. Rev.*, *137*, 149, doi:10.1007/s11214-008-9339-y.

Blatt, J. M., and V. F. Weisskopf (1979), *Theoretical Nuclear Physics*, Springer-Verlag New York.

Böhlen, T., F. Cerutti, M. Chin, A. Fassò, A. Ferrari, P. Ortega, A. Mairani, P. Sala, G. Smirnov, and V. Vlachoudis (2014), The fluka code: developments and challenges for high energy and medical applications, *Nuclear Data Sheets*, *120*, 211–214.

Bratolyubova-Tsulukidze, L., E. Grachev, O. Grigoryan, V. Kunitsyn, B. Kuzhevskij, D. Lysakov, O. Y. Nechaev, and M. Usanova (2004), Thunderstorms as the probable reason of high background neutron fluxes at l¡ 1.2, *Advances in Space Research*, *34*(8), 1815–1818.

Briggs, M. S., G. J. Fishman, V. Connaughton, P. N. Bhat, W. S. Paciesas, R. D. Preece, C. Wilson-Hodge, V. L. Chaplin, R. M. Kippen, A. von Kienlin, C. A. Meegan, E. Bissaldi, J. R. Dwyer, D. M. Smith, R. H. Holzworth, J. E. Grove, and A. Chekhtman (2010), First results on terrestrial gamma ray flashes from the Fermi Gamma-ray Burst Monitor, *Journal of Geophysical Research (Space Physics)*, *115*, A07323, doi: 10.1029/2009JA015242.

Briggs, M. S., V. Connaughton, C. Wilson-Hodge, R. D. Preece, G. J. Fishman, R. M. Kippen, P. Bhat, W. S. Paciesas, V. L. Chaplin, C. A. Meegan, et al. (2011), Electron-positron beams from terrestrial lightning observed with fermi gbm, *Geophysical research letters*, *38*(2).

Carlson, B., N. G. Lehtinen, and U. S. Inan (2010), Neutron production in terrestrial gamma ray flashes, *Journal of Geophysical Research: Space Physics*, *115*(A4).

Celestin, S., and V. P. Pasko (2011), Energy and fluxes of thermal runaway electrons produced by exponential growth of streamers during the stepping of lightning leaders and in transient luminous events, *Journal of Geophysical Research: Space Physics*, *116*(A3).

Celestin, S., W. Xu, and V. P. Pasko (2012), Terrestrial gamma ray flashes with energies up to 100 MeV produced by nonequilibrium acceleration of electrons in lightning, *Journal of Geophysical Research (Space Physics)*, *117*(16), A05315, doi:10.1029/2012JA017535.

Chanrion, O., and T. Neubert (2010), Production of runaway electrons by negative streamer discharges, *Journal of Geophysical Research: Space Physics*, *115*(A6).

Chanrion, O., Z. Bonaventura, D. Çinar, A. Bourdon, and T. Neubert (2014), Runaway electrons from a "beam-bulk" model of streamer: application to TGFs, *Environmental Research Letters*, *9*(5), 055003, doi:10.1088/1748-9326/9/5/055003.

Chilingarian, A., A. Daryan, K. Arakelyan, A. Hovhannisyan, B. Mailyan, L. Melkumyan, G. Hovsepyan, S. Chilingaryan, A. Reymers, and L. Vanyan (2010), Ground-based observations of thunderstorm-correlated fluxes of high-energy electrons, gamma rays, and neutrons, *Physical Review D*, *82*(4), 043,009.

Chilingarian, A., G. Hovsepyan, and A. Hovhannisyan (2011), Particle bursts from thunderclouds: Natural particle accelerators above our heads, *Physical review D*, *83*(6), 062,001.

Chilingarian, A., N. Bostanjyan, and L. Vanyan (2012), Neutron bursts associated with thunderstorms, *Physical review D*, *85*(8), 085,017.

Chilingarian, A., G. Hovsepyan, G. Khanikyanc, A. Reymers, and S. Soghomonyan (2015), Lightning origination and thunderstorm ground enhancements terminated by the lightning flash, *EPL (Europhysics Letters)*, *110*(4), 49,001.

Choi, H., R. Firestone, R. Lindstrom, G. L. Molnár, S. Mughabghab, Z. Revay, A. Trkov, V. Zerkin, and C. Zhou (2007), *Database of prompt gamma rays from slow neutron capture for elemental analysis*, International Atomic Energy Agency.

Cooray, V., L. Arevalo, M. Rahman, J. Dwyer, and H. Rassoul (2009), On the possible origin of x-rays in long laboratory sparks, *Journal of Atmospheric and Solar-Terrestrial*

Physics, *71*(17), 1890–1898.

Dietrich, S. S., and B. L. Berman (1988), Atlas of photoneutron cross sections obtained with monoenergetic photons, *Atomic Data and Nuclear Data Tables*, *38*(2), 199–338.

Drozdov, A., A. Grigoriev, and Y. Malyshkin (2013), Assessment of thunderstorm neutron radiation environment at altitudes of aviation flights, *Journal of Geophysical Research: Space Physics*, *118*(2), 947–955.

Dwyer, J. (2003), A fundamental limit on electric fields in air, *Geophysical Research Letters*, *30*(20).

Dwyer, J., Z. Saleh, H. Rassoul, D. Concha, M. Rahman, V. Cooray, J. Jerauld, M. Uman, and V. Rakov (2008a), A study of x-ray emission from laboratory sparks in air at atmospheric pressure, *Journal of Geophysical Research: Atmospheres*, *113*(D23).

Dwyer, J. R. (2007), Relativistic breakdown in planetary atmospheres, *Physics of Plasmas (1994-present)*, *14*(4), 042,901.

Dwyer, J. R. (2012), The relativistic feedback discharge model of terrestrial gamma ray flashes, *Journal of Geophysical Research: Space Physics*, *117*(A2).

Dwyer, J. R., B. W. Grefenstette, and D. M. Smith (2008b), High-energy electron beams launched into space by thunderstorms, *Geophysical Research Letters*, *35*(2).

Dwyer, J. R., D. M. Smith, and S. A. Cummer (2012), High-Energy Atmospheric Physics: Terrestrial Gamma-Ray Flashes and Related Phenomena, *ssr*, *173*, 133–196, doi:10.1007/s11214-012-9894-0.

Eack, K. B., W. H. Beasley, W. D. Rust, T. C. Marshall, and M. Stolzenburg (1996), Initial results from simultaneous observation of x-rays and electric fields in a thunderstorm,

Journal of Geophysical Research: Atmospheres, *101*(D23), 29,637–29,640.

Ferrari, A., P. R. Sala, A. Fasso, and J. Ranft (2005), Fluka: A multi-particle transport code (program version 2005), *Tech. rep.*

Fishman, G. J., P. Bhat, R. Mallozzi, J. Horack, T. Koshut, C. Kouveliotou, G. Pendleton, C. Meegan, R. Wilson, W. Paciesas, et al. (1994), Discovery of intense gamma-ray flashes of atmospheric origin, *Science*, *264*(5163), 1313–1316.

Fleischer, R. L., J. Plumer, and K. Crouch (1974), Are neutrons generated by lightning?, *Journal of Geophysical Research*, *79*(33), 5013–5017.

Gjesteland, T., N. Østgaard, S. Laviola, M. Miglietta, E. Arnone, M. Marisaldi, F. Fuschino, A. B. Collier, F. Fabró, and J. Montanya (2015), Observation of intrinsically bright terrestrial gamma ray flashes from the mediterranean basin, *Journal of Geophysical Research: Atmospheres*, *120*(23).

Gurevich, A. (1961), On the theory of runaway electrons, *Sov. Phys. JETP*, *12*(5), 904–912.

Gurevich, A., G. Milikh, and R. Roussel-Dupre (1992), Runaway electron mechanism of air breakdown and preconditioning during a thunderstorm, *Physics Letters A*, *165*(5), 463–468.

Gurevich, A., A. Chubenko, A. Karashtin, G. Mitko, A. Naumov, M. Ptitsyn, V. Ryabov, A. Shepetov, Y. V. Shlyugaev, L. Vildanova, et al. (2011), Gamma-ray emission from thunderstorm discharges, *Physics Letters A*, *375*(15), 1619–1625.

Gurevich, A., V. Antonova, A. Chubenko, A. Karashtin, G. Mitko, M. Ptitsyn, V. Ryabov, A. Shepetov, Y. V. Shlyugaev, L. Vildanova, et al. (2012), Strong flux of low-energy

neutrons produced by thunderstorms, *Physical review letters*, *108*(12), 125,001.

Gurevich, A., V. Antonova, A. Chubenko, A. Karashtin, O. Kryakunova, V. Y. Lutsenko, G. Mitko, V. Piskal, M. Ptitsyn, V. Ryabov, et al. (2015), The time structure of neutron emission during atmospheric discharge, *Atmospheric Research*, *164*, 339–346.

Kelley, N. A., D. M. Smith, J. R. Dwyer, M. Splitt, S. Lazarus, F. Martinez-McKinney, B. Hazelton, B. Grefenstette, A. Lowell, and H. K. Rassoul (2015), Relativistic electron avalanches as a thunderstorm discharge competing with lightning, *Nature communications*, *6*.

Kochkin, P., C. Nguyen, A. Van Deursen, and U. Ebert (2012), Experimental study of hard x-rays emitted from metre-scale positive discharges in air, *Journal of Physics D: Applied Physics*, *45*(42), 425,202.

Kochkin, P., A. Van Deursen, and U. Ebert (2015), Experimental study on hard x-rays emitted from metre-scale negative discharges in air, *Journal of Physics D: Applied Physics*, *48*(2), 025,205.

Kochkin, P., C. Köhn, U. Ebert, and L. van Deursen (2016), Analyzing x-ray emissions from meter-scale negative discharges in ambient air, *Plasma Sources Science and Technology*, *25*(4), 044,002.

Köhn, C., and U. Ebert (2015), Calculation of beams of positrons, neutrons, and protons associated with terrestrial gamma ray flashes, *Journal of Geophysical Research: Atmospheres*, *120*(4), 1620–1635.

Köhn, C., U. Ebert, and A. Mangiarotti (2014), The importance of electronelectron bremsstrahlung for terrestrial gamma-ray flashes, electron beams and electronpositron

beams, *Journal of Physics D: Applied Physics*, *47*(25), 252,001.

Köhn, C., O. Chanrion, and T. Neubert (2016), The influence of bremsstrahlung on electric discharge streamers in n2, o2 gas mixtures, *Plasma Sources Science and Technology*, *26*(1), 015,006.

Kostyrya, I., V. Tarasenko, A. Tkachev, and S. Yakovlenko (2006), X-ray radiation due to nanosecond volume discharges in air under atmospheric pressure, *Technical physics*, *51*(3), 356–361.

Kozlov, V., V. Mullayarov, S. Starodubtsev, and A. Toropov (2013), Neutron bursts during cloud-to-ground discharges of lightning, *Bulletin of the Russian Academy of Sciences: Physics*, *77*(5), 584–586.

Li, C., U. Ebert, and W. Hundsdorfer (2009), 3d hybrid computations for streamer discharges and production of runaway electrons, *Journal of Physics D: Applied Physics*, *42*(20), 202,003.

Mailyan, B., M. Briggs, E. Cramer, G. Fitzpatrick, O. Roberts, M. Stanbro, V. Connaughton, S. McBreen, P. Bhat, and J. Dwyer (2016), The spectroscopy of individual terrestrial gamma-ray flashes: Constraining the source properties, *Journal of Geophysical Research: Space Physics*, *121*(11).

Marisaldi, M., F. Fuschino, C. Pittori, F. Verrecchia, P. Giommi, M. Tavani, S. Dietrich, C. Price, A. Argan, C. Labanti, M. Galli, F. Longo, E. Del Monte, G. Barbiellini, A. Giuliani, A. Bulgarelli, F. Gianotti, M. Trifoglio, and A. Trois (2014), The first AGILE low-energy (¡ 30 MeV) Terrestrial Gamma-ray Flashes catalog, in *EGU General Assembly Conference Abstracts*, *EGU General Assembly Conference Abstracts*, vol. 16,

p. 11326.

McCarthy, M., and G. Parks (1985), Further observations of x-rays inside thunderstorms, *Geophysical research letters*, *12*(6), 393–396.

Moss, G. D., V. P. Pasko, N. Liu, and G. Veronis (2006), Monte Carlo model for analysis of thermal runaway electrons in streamer tips in transient luminous events and streamer zones of lightning leaders, *Journal of Geophysical Research (Space Physics)*, *111*, A02307, doi:10.1029/2005JA011350.

Nguyen, C. V., A. P. van Deursen, and U. Ebert (2008), Multiple x-ray bursts from long discharges in air, *Journal of Physics D: Applied Physics*, *41*(23), 234,012.

Noggle, R., E. Krider, and J. Wayland (1968), A search for x rays from helium and air discharges at atmospheric pressure, *Journal of Applied Physics*, *39*(10), 4746–4748.

Oblozinskỳ, P. (2000), Handbook of photonuclear data for applications: Cross sections and spectra, *International Atomic Energy Association report IAEA-TECDOC-1178, Vienna, Austria*.

Rep'ev, A., and P. Repin (2008), Spatiotemporal parameters of the x-ray radiation from a diffuse atmospheric-pressure discharge, *Technical Physics*, *53*(1), 73–80.

Rutjes, C., D. Sarria, A. B. Skeltved, A. Luque, G. Diniz, N. Østgaard, and U. Ebert (2016), Evaluation of monte carlo tools for high energy atmospheric physics, *Geoscientific Model Development*, *9*(11), 3961.

Shah, G., H. Razdan, C. Bhat, and Q. Ali (1985), Neutron generation in lightning bolts.

Shao, T., C. Zhang, Z. Niu, P. Yan, V. F. Tarasenko, E. K. Baksht, A. G. Burahenko, and Y. V. Shutko (2011), Diffuse discharge, runaway electron, and x-ray in atmospheric

pressure air in an inhomogeneous electrical field in repetitive pulsed modes, *Applied Physics Letters*, *98*(2), 021,503.

Shyam, A., and T. Kaushik (1999), Observation of neutron bursts associated with atmospheric lightning discharge, *Journal of Geophysical Research: Space Physics*, *104*(A4), 6867–6869.

Stankevich, Y. L., and V. Kalinin (1967), Fast electrons and x radiation during the initial stages of an impulse spark discharge in air., *Dokl. Akad. Nauk SSSR, 177: 72-3 (Nov.-Dec. 1967).*

Starodubtsev, S. A., V. Kozlov, A. Toropov, V. Mullayarov, V. G. Grigorev, and A. Moiseev (2012), First experimental observations of neutron bursts under thunderstorm clouds near sea level, *JETP letters*, *96*(3), 188–191.

Tarasenko, V. F., E. K. Baksht, A. G. Burachenko, I. D. Kostyrya, M. I. Lomaev, and D. V. Rybka (2008), Generation of supershort avalanche electron beams and formation of diffuse discharges in different gases at high pressure, *Plasma Devices and Operations*, *16*(4), 267–298.

Torii, T., M. Takeishi, and T. Hosono (2002), Observation of gamma-ray dose increase associated with winter thunderstorm and lightning activity, *Journal of Geophysical Research: Atmospheres*, *107*(D17).

Toropov, A., V. Kozlov, V. Mullayarov, and S. Starodubtsev (2013), Experimental observations of strengthening the neutron flux during negative lightning discharges of thunderclouds with tripolar configuration, *Journal of Atmospheric and Solar-Terrestrial Physics*, *94*, 13–18.

Tsuchiya, H., T. Enoto, S. Yamada, T. Yuasa, M. Kawaharada, T. Kitaguchi, M. Kokubun, H. Kato, M. Okano, S. Nakamura, et al. (2007), Detection of high-energy gamma rays from winter thunderclouds, *Physical review letters*, *99*(16), 165,002.

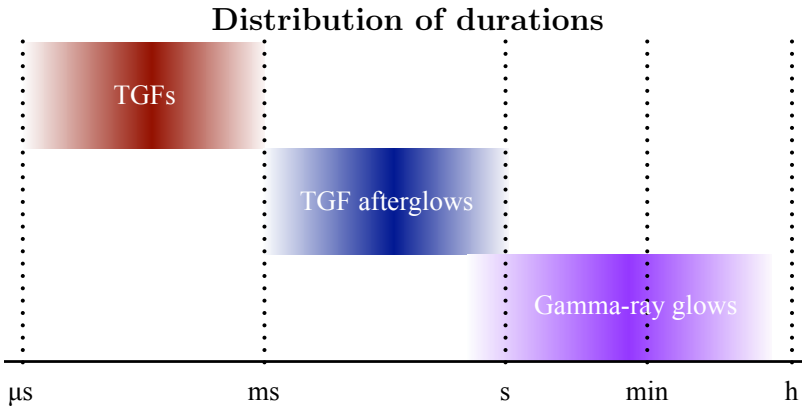

Figure 1. Sketch of the distribution of durations of TGFs, TGF afterglows and gamma-ray glows.

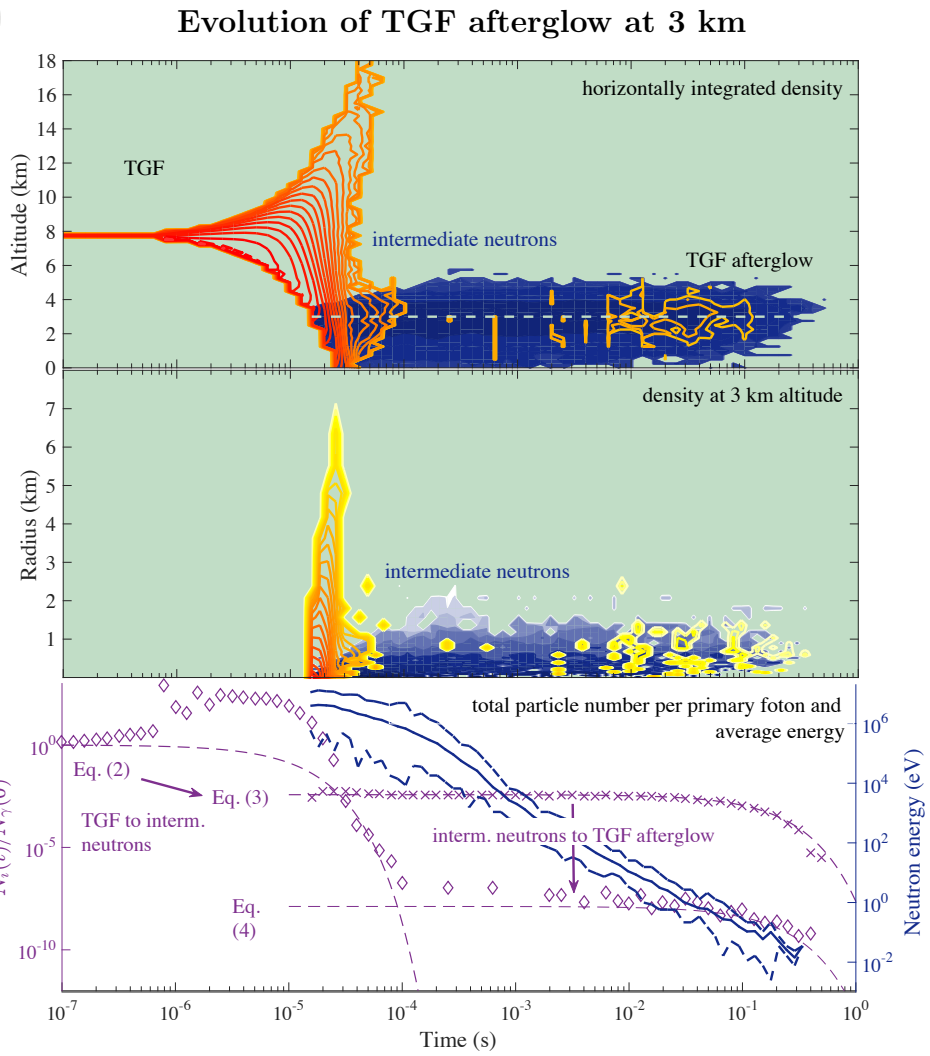

Figure 2. Evolution of the TGF afterglow generated by the primary TGF as a function of the logarithm of time. Top and middle panel are contour figures of the photon and neutron density (see definitions in Sec. 2.1), on a logarithmic scale; contours represent half a decade (i.e. a factor of $10^{0.5}$). The contour lines (red, yellow to white) are photons above 10 keV, the filled contours (blue to white) are neutrons. In the top panel the density is horizontally integrated. The middle panel gives the density profile as a function of radius at 3 km altitude, the density is averaged over rings around the symmetry axis. The bottom panel shows two quantities: on the left y-axis in purple the total particle number $N_i(t)$ of photons (diamonds) and neutrons (crosses), per initial photon $N_\gamma(0)$, with their approximations given by equations (2), (3) and (4); on the right y-axis in blue the average neutron energy is drawn as a solid line, together with the minimal and the maximal neutron energy as dashed lines.

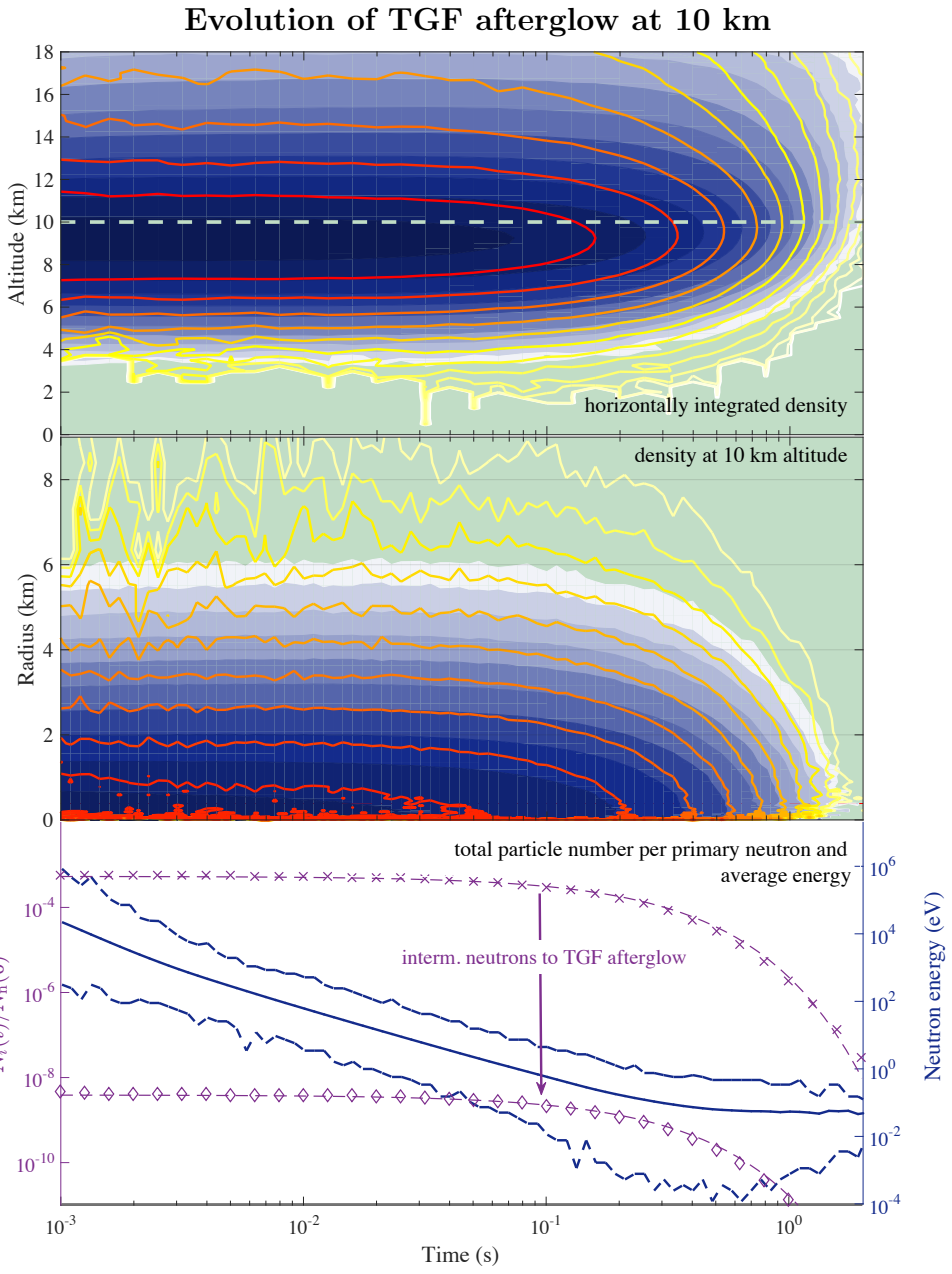

Figure 3. The same as in Fig. 2, but now for the TGF afterglow started from a neutron source at 10 km directed downwards. In this figure time is plotted only from 10^{-3} s on, focussing on the TGF afterglow. The bottom panel does not represent the total particle number as some escaped of the system at the upper boundary at 18 km, see text. The decay rates, i.e., the fits of the purple dashed lines, are the same as in Fig. 2, adapted to the lower air density (at 10 km compared to 3 km).

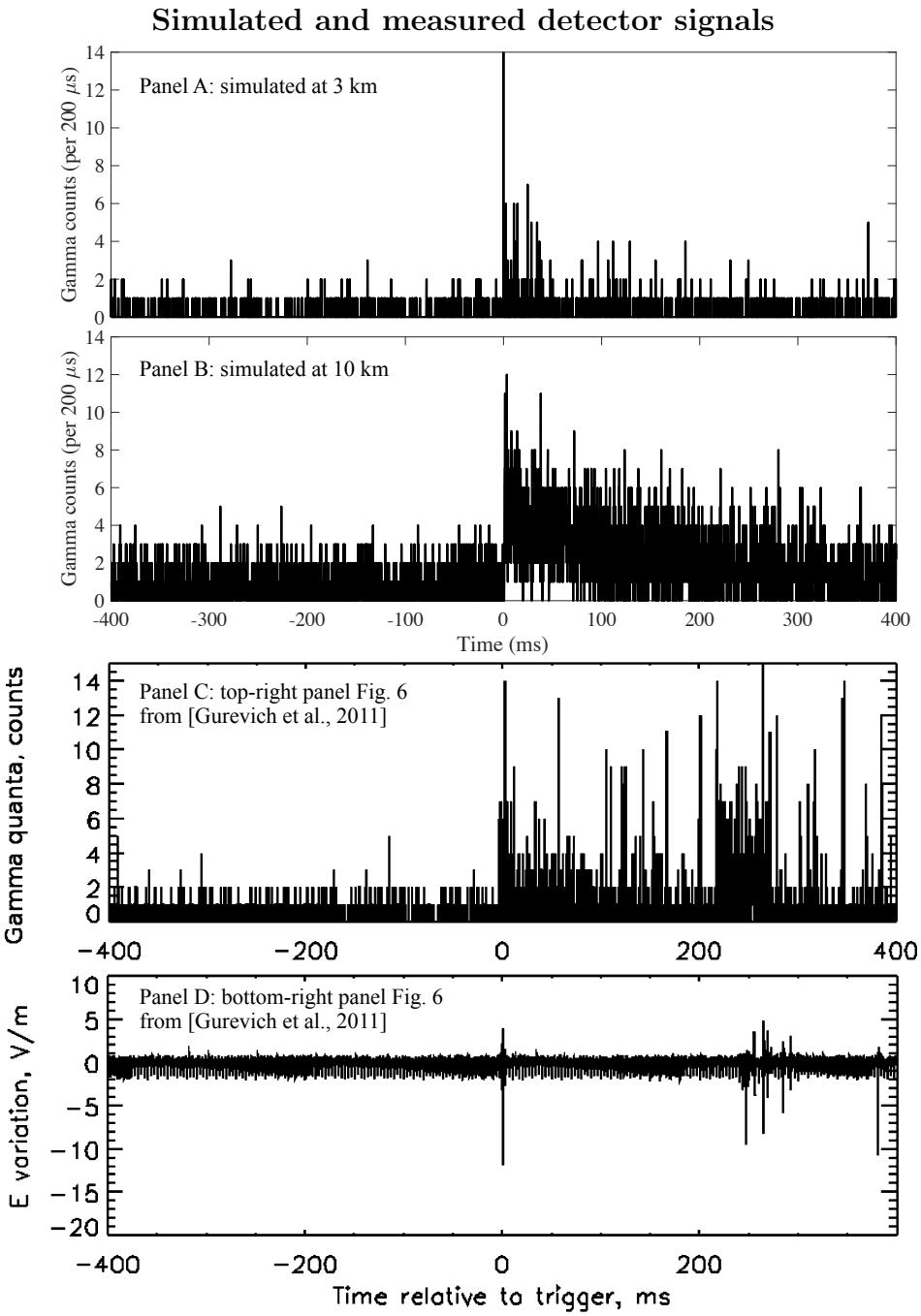

Figure 4. Panel A and B: simulated counts of gamma-radiation, from the simulation presented in Fig. 2 and Fig. 3. Panel C and D are taken from [*Gurevich et al.*, 2011], in which it is denoted there as event "6". Panel A to C are gamma-ray counts per 200 μs interval on a detector of 475 cm^2, at 3, 10 and 3.8 km respectively. Panel D gives the measured fast electric field variation (20 μs sampling rate measured by the capacity sensor, see for more details [*Gurevich et al.*, 2011]).